Constraining the cosmic strings gravitational wave spectra in no-scale inflation with viable gravitino dark matter and nonthermal leptogenesis

Waqas Ahmed,[1,*] M. Junaid,[2,†] Salah Nasri,[3,4,‡] and Umer Zubair[5,§]

[1]*School of Mathematics and Physics, Hubei Polytechnic University, Huangshi 435003, China*
[2]*National Centre for Physics, Islamabad 44000, Pakistan*
[3]*Department of Physics, United Arab Emirates University, Al Ain 15551 Abu Dhabi, United Arab Emirates*
[4]*International Center for Theoretical Physics, Trieste I–34151, Italy*
[5]*Department of Physics and Astronomy, University of Delaware, Newark, Delaware 19716, USA*

(Received 29 March 2022; accepted 23 May 2022; published 3 June 2022)

We revisit the hybrid inflation model gauged by $U(1)_{B-L}$ extension of the minimal supersymmetric standard model in a no-scale background. Considering a single predictive framework, we study inflation, leptogenesis, gavitino cosmology, and the stochastic background of gravitational waves produced by metastable cosmic strings. The spontaneous breaking of $U(1)_{B-L}$ at the end of inflation produces a network of metastable cosmic strings, while the interaction between the $U(1)_{B-L}$ Higgs field and the neutrinos generate heavy Majorana masses for the right-handed neutrinos. The heavy Majorana masses explain the tiny neutrino masses via the seesaw mechanism, a realistic scenario for reheating and nonthermal leptogenesis. We show that a successful nonthermal leptogenesis and a stable gravitino as a dark matter candidate can be achieved for a wide range of reheating temperatures and $U(1)_{B-L}$ symmetry breaking scales. The possibility of realizing metastable cosmic strings in a grand unified theory setup is briefly discussed. We find that a successful reheating with nonthermal leptogenesis and gravitino dark matter restricts the allowed values of string tension to a narrow range $10^{-9} \lesssim G\mu_{CS} \lesssim 8 \times 10^{-6}$, predicting a stochastic gravitational-wave background that lies within the 1σ bounds of the recent NANOGrav 12.5-yr data, as well as within the sensitivity bounds of future GW experiments.

DOI: 10.1103/PhysRevD.105.115008

I. INTRODUCTION

Spontaneous symmetry breaking in grand unified theories (GUTs) can produce a variety of topological or nontopological defects [1–5]. These defects generically arise from the breaking of a group G to its subgroup H, such that a manifold of equivalent vacua, $\mathcal{M}$, G/H, exists. Monopoles form when the manifold $\mathcal{M}$ contains noncontractible two-dimensional spheres [6], cosmic strings when it contains noncontractible loops, and domain walls when $\mathcal{M}$ is disconnected [7]. The monopoles can be avoided by inflation, which naturally incorporates the GUT scale in supersymmetric hybrid inflation [8]. It has been shown for a large class of GUT models that in spontaneous symmetry breaking schemes curing the monopole problem, the formation of cosmic strings cannot be avoided [9].

Cosmic strings are interesting messengers from the early Universe due to their characteristic signatures in the stochastic gravitational wave background (SGWB). The evidence for a stochastic process at nanohertz frequencies as reported by recent NANOGrav 12.5 year data has been interpreted as SGWB in a large number of recent papers [10–20]. Relic gravitational waves (GWs) provide a fascinating window to explore the very early Universe cosmology [21]. Cosmic strings produce powerful bursts of gravitational radiation that could be detected by interferometric gravitational wave detectors such as LIGO, Virgo, and LISA [22,23]. In addition, the stochastic gravitational wave background can be detected or constrained by various observations including big bang nucleosynthesis (BBN), pulsar timing experiments, and interferometric gravitational wave detectors [24].

Among the various proposed extensions of the minimal supersymmetric standard model (MSSM), the $U(1)_{B-L}$ is the simplest [25–27]. Here B and L denote the baryon and lepton numbers, respectively, and $B-L$ is the difference between baryon and lepton numbers. As a local symmetry, the $B-L$ group resides in the grand unified gauge group

*waqasmit@hbpu.edu.cn
†mjunaid@ualberta.ca
‡snasri@uaeu.ac.ae; salah.nasri@cern.ch
§umer@udel.edu

Published by the American Physical Society under the terms of the Creative Commons Attribution 4.0 International license. Further distribution of this work must maintain attribution to the author(s) and the published article's title, journal citation, and DOI. Funded by SCOAP³.

$SO(10)$. The spontaneous breaking of $U(1)_{B-L}$ at the end of inflation requires an extended scalar sector, which automatically yields hybrid inflation explaining the inhomogeneities of the cosmic microwave background (CMB). In the $B-L$ breaking phase transition, most of the vacuum energy density is rapidly transferred to nonrelativistic $B-L$ Higgs bosons, a sizable fraction also into cosmic strings. The decay of heavy Higgs bosons and heavy neutrinos leads to an elegant explanation of the small neutrino masses via the seesaw mechanism, explaining the baryon asymmetry via thermal and nonthermal leptogenesis [28–31]. The temperature evolution during reheating is controlled by the interplay between the $B-L$ Higgs and the neutrino sector, while the dark matter originates from thermally produced gravitinos. The embedding of $U(1)_{B-L}$ into a simply connected group such as $SO(10)$ or Pati-salam symmetry ($SU(4)_C \times SU(2)_L \times SU(2)_R$), produces metastable cosmic strings due to the spontaneous pair creation of a monopole and an antimonopole. Once the string is cut, the monopoles at the two ends are quickly pulled together due to string tension, forcing them to annihilate. If the string network is sufficiently long-lived, it can generate a stochastic gravitational wave background in the range of ongoing and future gravitational wave experiments [32,33].

Hybrid inflation, in particular, is one of the most promising models of inflation, and can be naturally realized within the context of supergravity theories. This scenario is based on the inclusion of two scalar fields [34], with the first one realizing the slow-roll inflation and the second one, dubbed the "waterfall" field, triggering the end of an inflationary epoch. While in the standard hybrid inflationary scenario [8,35,36], the GUT gauge symmetry is broken at the end of inflation, in shifted [37] and smooth variants [38,39], the gauge symmetry breaking occurs during inflation and thus the disastrous magnetic monopoles and other dangerous topological defects are inflated away.

In this paper we study standard hybrid inflation in the context of supergravity where a no-scale Kähler potential is assumed. We consider the framework of MSSM gauge symmetry augmented by a $U(1)_{B-L}$ factor and investigate the implementation of hybrid inflation and its interplay with the issues of nonthermal leptogenesis, gravitino dark matter and stochastic gravitational wave background generated by metastable cosmic string network. For μ hybrid inflation see Ref. [40]. We consider the value of monopole-string-tension ratio from $\sqrt{\lambda} \simeq 7.4$ (metastable cosmic strings) to $\sqrt{\lambda} \simeq 9.0$ (quasistable cosmic strings). The parametric space consistent with successful reheating with nonthermal leptogenesis and gravitino dark matter restrict the allowed values of string tension to the range $10^{-9} \lesssim G\mu_{CS} \lesssim 8 \times 10^{-6}$ and predicts a stochastic gravitational wave background that lies within the 1σ and 2σ bounds of recent NANOGrav 12.5- data, as well as the sensitivity bounds of future gravitational wave experiments.

The layout of the paper is as follows. In Sec. II we describe the basic features of the model including the superfields, their charge assignments, and the superpotential constrained by a $U(1)_R$ symmetry. The inflationary setup is described in Sec. III. The numerical analysis is presented in Sec. IV including the prospects of observing primordial gravity waves, nonthermal leptogenesis, gravitino cosmology, and stochastic gravitational wave background generated by metastable cosmic string network. Our conclusion is summarized in Sec. V.

II. MODEL DESCRIPTION

In this section, we present basic features regarding the gauge symmetry and the spectrum of the effective model in which the inflationary scenario will be implemented. The gauge group $U(1)_{B-L}$ is embedded in a grand unified gauge group $SO(10)$ and is based on the gauge symmetry

$$G_{B-L} = SU(3)_C \times SU(2)_L \times U(1)_Y \times U(1)_{B-L}. \quad (1)$$

In addition to the MSSM matter and Higgs superfields, the model supplements six superfields; namely, a gauge singlet S whose scalar component acts as inflaton, three right-handed neutrinos N_i^c, and a pair of Higgs singlets H and $\bar{H}$, which are responsible for breaking the gauge group $U(1)_{B-L}$. The charge assignment of these superfields under the gauge symmetry $SU(3)_C \times SU(2)_L \times U(1)_Y \times U(1)_{B-L}$ as well as the global symmetries $U(1)_R$, $U(1)_B$, and $U(1)_L$ are listed in Table I.

The $U(1)_{B-L}$ symmetry is spontaneously broken when the H, $\bar{H}$ singlet Higgs superfields acquire vacuum expectation values (VEVs), providing Majorana masses to the right-handed neutrinos. The superpotential of the model, invariant under the symmetries listed in Table I, is given as

$$\begin{aligned} W = {} & \mu H_u H_d + y_u H_u Q u^c + y_d H_d Q d^c + y_e H_d L e^c \\ & + y_\nu H_u L N^c + \kappa S(\bar{H}H - M^2) + \beta'_{ij} \frac{HHN^cN^c}{\Lambda}. \end{aligned} \quad (2)$$

The first line in the above superpotential contains the usual MSSM μ term and Yukawa couplings supplemented by an additional Yukawa coupling among L_i and N_i^c. These Yukawa couplings generate Dirac masses for up and down quarks, charged leptons, and neutrinos. The family indices for Yukawa couplings are generally suppressed for simplicity. The first term in the second line is relevent for standard supersymmetric hybrid inflation with M being a GUT scale mass parameter and κ a dimensionless coupling constant. The nonrenormalizable term in the second line generates Majorana masses for right-handed neutrinos N_i^c and induces the decay of inflaton to N_i^c. By virtue of the extra

TABLE I. Superfield contents of the model, the corresponding representations under the local gauge symmetry G_{B-L}, and the properties with respect to the extra global symmetries, $U(1)_R$, $U(1)_B$, and $U(1)_L$.

Superfields	Representations under G_{B-L}	Global symmetries		
		$U(1)_R$	B	L
Matter fields				
e_i^c	$(\mathbf{1},\mathbf{1},1,1)$	1	0	−1
N_i^c	$(\mathbf{1},\mathbf{1},0,1)$	1	0	−1
L_i	$(\mathbf{1},\mathbf{2},-1/2,-1)$	0	0	1
u_i^c	$(\mathbf{3},\mathbf{1},-2/3,-1/3)$	1/2	−1/3	0
d_i^c	$(\mathbf{3},\mathbf{1},1/3,-1/3)$	1/2	−1/3	0
Q_i	$(\bar{\mathbf{3}},\mathbf{2},1/6,1/3)$	1/2	1/3	0
Higgs fields				
H_d	$(\mathbf{1},\mathbf{2},-1/2,0)$	1	0	0
H_u	$(\mathbf{1},\mathbf{2},1/2,0)$	1	0	0
S	$(\mathbf{1},\mathbf{1},0,0)$	2	0	0
$\bar{H}$	$(\mathbf{1},\mathbf{1},0,1)$	0	0	−1
H	$(\mathbf{1},\mathbf{1},0,-1)$	0	0	1

global symmetries, the model is protected from dangerous proton decay operators and R-parity violating terms.

III. INFLATION POTENTIAL

We will compute the effective scalar potential contributions from the F- and D-sector radiative corrections as well as the soft supersymmetry breaking terms. The superpotential terms relevant for inflation are

$$W \supset \kappa S(\bar{H}H - M^2). \tag{3}$$

We consider a no-scale structure Kähler potential which, after including contributions from the relevant fields in the model, takes the following form:

$$K = -3m_P^2 \log\left[T + T^* - \frac{1}{3m_P^2}(HH^* + \bar{H}\bar{H}^* + S^\dagger S) + \frac{\xi}{3m_P^2}(H\bar{H} + H^*\bar{H}^*) + \frac{\gamma}{3m_P^4}(S^\dagger S)^2 + \cdots\right], \tag{4}$$

where T, T^* are Kähler complex moduli fields, $T = (u + iv)$, hence $T + T^* = 2u$ and ξ is a dimensionless parameter. Here we choose $u = 1/2$. For later convenience, we define

$$\Delta = \left[T + T^* - \frac{1}{3m_P^2}(HH^* + \bar{H}\bar{H}^* + S^\dagger S) + \frac{\xi}{3m_P^2}(H\bar{H} + H^*\bar{H}^*) + \frac{\gamma}{3m_P^4}(S^\dagger S)^2 + \cdots\right], \tag{5}$$

so that Eq. (4) can be written as

$$K = -3m_P^2 \log \Delta. \tag{6}$$

The fields carrying $SU(3)_C \times SU(2)_L \times U(1)_Y \times U(1)_{B-L}$ quantum numbers are given in Table I and denoted collectively here with ϕ_i. The D-term potential is given as

$$V_D = \frac{1}{2} D_a^p D_a^p, \tag{7}$$

where D_a^p is defined for $SU(N)$ groups as

$$D_a^p = -g_a K_{,\phi_i}[t_a^p]_i^j \phi_j$$

and for $U(1)$ groups as

$$D_a^p = -g_a K_{,\phi_i}[t_a^p]_i^j \phi_j - g_a q_i \varsigma.$$

Here $K_{,\phi_i} \equiv dK/d\phi_i$, ς is the Fayet-Iliopoulos coupling constant and q_i are the charges under the $U(1)$ group. The t_a^p are the generators of the corresponding group G and $p = 1, \ldots, \dim(G)$. The D-term potential can be written as

$$V_D = \frac{g_{B-L}^2}{2\Delta^2}[2|\bar{H}|^2 - 2|H|^2 - \xi(2H\bar{H} - 2\bar{H}H) + (q_H + q_{\bar{H}})\varsigma]^2. \tag{8}$$

The D-flat potential can be achieve by parametrization of the fields H and $\bar{H}$. We can rewrite the complex fields in terms of real scalar fields as

$$H = \frac{Y}{\sqrt{2}} e^{\imath\theta} \cos\vartheta, \qquad \bar{H} = \frac{Y}{\sqrt{2}} e^{\imath\bar{\theta}} \sin\vartheta, \tag{9}$$

where the phases θ, $\bar{\theta}$, and ϑ can be stabilized at

$$\vartheta = \frac{\pi}{4} \quad \text{and} \quad \theta = \bar{\theta} = 0 \tag{10}$$

along the D-flat direction ($|H| = |\bar{H}| = \frac{Y}{2}$). The F-term SUGRA scalar potential is given by

$$V_F = e^{K/m_P^2}\left[(K_{i\bar{j}})^{-1}(D_{z_i}W)(D_{z_j}W)^* - \frac{3|W|^2}{m_P^2}\right], \tag{11}$$

with z_i being the bosonic components of the superfields $z_i \in \{S, H, \bar{H}, \cdots\}$, and we have defined

$$D_{z_i}W \equiv \frac{\partial W}{\partial z_i} + \frac{\partial K}{\partial z_i}\frac{W}{m_p^2}, \qquad K_{i\bar{j}} \equiv \frac{\partial^2 K}{\partial z_i \partial z_j^*}, \tag{12}$$

and $D_{z_i^*}W^* = (D_{z_i}W)^*$. The F-term scalar potential during inflation becomes

$$V_F(Y,|S|) = \frac{\kappa^2}{16}(Y^2-4M^2)^2 + \kappa^2 Y^2|S|^2 - \kappa^2 M^4\left(\frac{2}{3}-4\gamma\right)\left(\frac{|S|}{m_p}\right)^2 + \kappa^2 M^4\left(-\frac{5}{9}+\frac{14\gamma}{3}+16\gamma^2\right)\left(\frac{|S|}{m_p}\right)^4\cdots. \quad (13)$$

Using the F-flatness condition $D_{z_i}W = 0$, the minima of potential lies at $Y = 2M$ and $S = 0$. Along the inflationary trajectory, $Y = 0$, the gauge group $U(1)_{B-L}$ is unbroken. After the end of inflation, the spontaneous breaking of the gauge group $U(1)_{B-L}$ yields cosmic strings. Defining dimensionless variable $x \equiv |S|/M$, we obtain the following form of potential along the inflationary trajectory,

$$V_F(x) \simeq \kappa^2 M^4\left(1-\left(\frac{2}{3}-4\gamma\right)\left(\frac{Mx}{m_p}\right)^2 + \left(-\frac{5}{9}+\frac{14\gamma}{3}+16\gamma^2\right)\left(\frac{Mx}{m_p}\right)^4+\cdots\right). \quad (14)$$

The action of our model for noncanonically normalized field x is given by

$$\mathcal{A} = \int dx^4\sqrt{-g}\left[\frac{m_p^2}{2}\mathcal{R} - K^i_j\partial_\mu x^i\partial^\mu x^j - V(x)\right]. \quad (15)$$

Introducing a canonically normalized field χ that satisfies

$$\left(\frac{d\chi}{dx}\right)^2 = \frac{3\frac{\gamma M^2}{m_p^2}x^2(\frac{M^2}{m_p^2}x^2-12)+9}{(\frac{M^2}{m_p^2}x^2(\frac{\gamma M^2}{m_p^2}x^2-1)+3)^2} \sim 1. \quad (16)$$

Since $\gamma M^2 \ll m_p^2$, integrating Eq. (16) in this limit, we obtain the canonically normalized field χ as a function of x. The canonically normalized potential as a function of χ can be written as

$$V_F(\chi) \simeq \kappa^2 M^4\left(1-\left(\frac{2}{3}-4\gamma\right)\left(\frac{M}{m_p}\right)^2\chi^2 + \left(-\frac{5}{9}+\frac{14\gamma}{3}+16\gamma^2\right)\left(\frac{M}{m_p}\right)^4\chi^4+\cdots\right). \quad (17)$$

The effective scalar potential including the well-known radiative corrections and soft SUSY breaking terms can be expressed as

$$V(\chi) \simeq V_F + V_D + V_{CW} + V_{\text{Soft}} \quad (18)$$

$$\simeq \kappa^2 M^4\left(1-\left(\frac{2}{3}-4\gamma\right)\left(\frac{M}{m_p}\right)^2\chi^2 + \left(-\frac{5}{9}+\frac{14\gamma}{3}+16\gamma^2\right)\left(\frac{M}{m_p}\right)^4 + \frac{\kappa^2}{8\pi^2}F(\chi) + a\left(\frac{m_{3/2}\chi}{\kappa M}\right) + \left(\frac{M_S\chi}{\kappa M}\right)^2\right), \quad (19)$$

with

$$a = 2|A-2|\cos[\arg S + \arg(1-A)], \quad (20)$$

and

$$F(\chi) = \frac{1}{4}\left((\chi^4+1)\log\left(\frac{\chi^4-1}{\chi^4}\right) + 2\chi^2\log\left(\frac{\chi^2+1}{\chi^2-1}\right) + 2\log\left(\frac{\kappa^2M^2\chi^2}{Q^2}\right) - 3\right). \quad (21)$$

Here, Q is the renormalization scale, a and M_S are the coefficients of soft SUSY breaking linear and mass terms for S, respectively, and $m_{3/2}$ is the gravitino mass. For simplicity, we set $M_S = m_{3/2}$ and assume a suitable initial condition for $\arg S$ to be stabilized at zero and take a to be constant during inflation (for details see Ref. [41]).

IV. ANALYSIS

In this section, we analyze the implications of the model and discuss its predictions regarding the various cosmological observables. We pay particular attention to inflationary predictions and stochastic gravitational waves spectrum consistent with leptogenesis and gravitino cosmology.

A. Inflationary predictions

The inflationary slow-roll parameters can be expressed in terms of χ as

$$\epsilon = \frac{1}{4}\left(\frac{m_p}{M}\right)^2\left(\frac{V'(\chi)}{V(\chi)}\right)^2, \quad \eta = \frac{1}{2}\left(\frac{m_p}{M}\right)^2\left(\frac{V''(\chi)}{V(\chi)}\right), \quad (22)$$

$$s^2 = \frac{1}{4}\left(\frac{m_p}{M}\right)^4\left(\frac{V'(\chi)V''(\chi)}{V(\chi)}\right), \quad (23)$$

where a prime denotes a derivative with respect to χ. The tensor-to-scalar ratio r, the scalar spectral index n_s, and the running of the spectral index $\frac{dn_s}{d\ln k}$ are given by

$$r \simeq 16\epsilon, \;\; n_s \simeq 1+2\eta-6\epsilon, \;\; \frac{dn_s}{d\ln k} \simeq 16\epsilon\eta - 24\epsilon^2 + 2s^2. \quad (24)$$

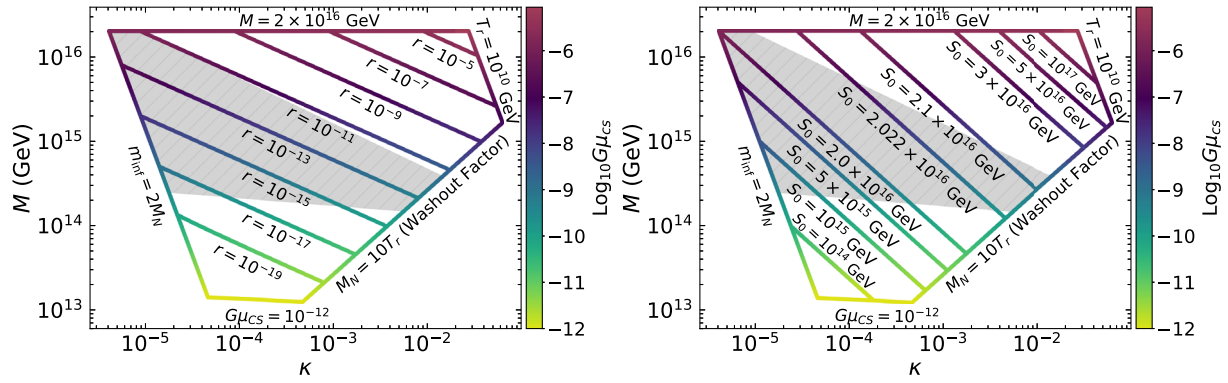

FIG. 1. Contours of tensor to scalar ratio r (left panel) and the field S_0 (right panel) in the κ–M plane, where M is the $B-L$ gauge symmetry breaking scale. The boundary is drawn for different constraints shown. The color bar on the right displays the range of string tension parameter $G\mu_{CS}$. The shaded region represents the parametric space that is consistent with gravitino dark matter.

The number of e-folds is given by [42],

$$N_l = 2\left(\frac{M}{m_p}\right)^2 \int_{\chi_e}^{\chi_l} \left(\frac{V(\chi)}{V'(\chi)}\right) d\chi = 54 + \frac{1}{3}\ln\left[\frac{T_r}{10^9\ \mathrm{GeV}}\right] + \frac{1}{3}\ln\left[\frac{V(\chi_l)^{1/4}}{10^{16}\ \mathrm{GeV}}\right], \quad (25)$$

where l denotes the comoving scale after crossing the horizon, χ_l is the field value at l, χ_e is the field value at the end of inflation, (i.e., when $\epsilon = 1$), and T_r is the reheating temperature, which will be discussed in the following section. The amplitude of curvature perturbation Δ_R is given by

$$\Delta_R^2 = \frac{V(\chi)}{24\pi^2\epsilon(\chi)}. \quad (26)$$

The results of our numerical calculations are presented in Fig. 1, where the variation of parameters is shown in the κ–M plane. In our analysis, the scalar spectral index is fixed at the central value of Planck's bounds $n_s = 0.9655$. To keep the SUGRA expansion, parametrized by γ, under control we impose $S_0 \leq m_p$. We restrict $M \leq 2 \times 10^{16}$ and $T_r \leq 10^{10}$ GeV to avoid the gravitino problem. We further restrict our numerical results by imposing the following conditions

$$m_{\mathrm{inf}} = 2M_N, \qquad M_N = 10T_r, \quad (27)$$

which ensure successful reheating with nonthermal leptogenesis. The boundary curves in Fig. 1 represent $M = 2 \times 10^{16}$ GeV, $T_r = 10^{10}$ GeV, $m_{\mathrm{inf}} = 2M_N$, $M_N = 10T_r$, and $G\mu = 10^{-12}$ constraints. The left panel in Fig. 1 shows the variation of tensor to scalar ratio r, whereas the right panel shows the variation of the field value S_0. The color bar depicts the range of string tension $G\mu_{CS}$ obtained in our model. It should be noted that the parameter γ which controls the SUGRA corrections, makes this model more predictive than the standard hybrid model of inflation. Using leading order slow-roll approximation, we obtain the following analytical expressions for n_s in the small κ limit,

$$n_s = 1 - 2\left(\frac{2}{3} - 4\gamma\right). \quad (28)$$

It can readily be checked that for $\gamma = 0.162292$, we obtain $n_s \sim 0.9655$ which is in excellent agreement with the numerical results displayed in Fig. 1. The above equation therefore gives a valid approximation of our numerical results. For the scalar spectral index n_s fixed at Planck's central value (0.9655), we obtain the following ranges of parameters:

$$\begin{aligned} 4.2 \times 10^{-6} \lesssim \kappa \lesssim 6.2 \times 10^{-2}, \\ (1.3 \times 10^{13} \lesssim M \lesssim 2.0 \times 10^{16})\ \mathrm{GeV}, \\ (2 \times 10^{16} \lesssim S_0 \lesssim 2 \times 10^{17})\ \mathrm{GeV}, \\ 7.1 \times 10^{-23} \lesssim r \lesssim 10^{-4}, \\ 10^{-12} \lesssim G\mu_{CS} \lesssim 8 \times 10^{-6}. \end{aligned} \quad (29)$$

Using the Planck's normalization constraint on Δ_R, we obtain the following explicit dependence of r on κ and M:

$$r \simeq \frac{2\kappa^2}{3\pi^2\Delta_R^2}\left(\frac{M}{m_P}\right)^4, \quad (30)$$

which explains the behavior of tensor to scalar ratio r in κ–M plane. It can readily be checked that for $\kappa \simeq 4.65 \times 10^{-5}$ and $M \simeq 1.42 \times 10^{13}$ GeV, the above equation gives $r \simeq 7.9 \times 10^{-23}$. On the other hand, $\kappa \simeq 2.7 \times 10^{-2}$ and $M \simeq 2.0 \times 10^{16}$ GeV gives $r \simeq 10^{-4}$. These approximate values are very close to the actual values obtained in the numerical calculations.

B. Reheating with nonthermal leptogenesis

At the end of the inflation epoch, the vacuum energy is transferred to the energies of coherent oscillations of the inflaton S and the scalar field $\theta = (\delta H + \delta\bar{H})/\sqrt{2}$ whose decays give rise to the radiation in the Universe. The inflaton decay to right-handed neutrino is induced by the superpotential term

$$W \supset \beta'_{ij}\frac{HHN^cN^c}{\Lambda}, \tag{31}$$

where β'_{ij} is a coupling constant and Λ represents a high cutoff scale (in a string model this could be identified with the compactification scale). Heavy Majorana masses for the right-handed neutrinos are provided by the term

$$M_{\nu^c_{ij}} = \beta'_{ij}\frac{\langle H\rangle\langle H\rangle}{\Lambda}. \tag{32}$$

Also, Dirac neutrino masses of the order of the electroweak scale are obtained from the tree-level superpotential term $y_{\nu ij}N^c_i L_j H_u \to m_{\nu_D ij}NN^c$ given in (2). Thus, the neutrino sector is

$$W \supset m_{\nu_D ij}N_iN^c_j + M_{\nu^c_{ij}}N^c_iN^c_j. \tag{33}$$

The small neutrino masses supported by neutrino oscillation experiments, are obtained by integrating out the heavy right-handed neutrinos and read as

$$m_{\nu_D\alpha\beta} = -\sum_i y_{\nu i\alpha}y_{\nu i\beta}\frac{v_u^2}{M_i}. \tag{34}$$

The neutrino mass matrix $m_{\nu_D\alpha\beta}$ can be diagonalized by a unitary matrix $U_{\alpha i}$ as $m_{\nu_D\alpha\beta} = U_{\alpha i}U_{\beta i}m_{\nu_D}$, where m_{ν_D} is a diagonal mass matrix $m_{\nu_D} = \mathrm{diag}(m_{\nu_1}, m_{\nu_2}, m_{\nu_3})$ and M_i represent the eigenvalue of mass matrix $M_{\nu^c_{ij}}$.

The lepton asymmetry is generated (inducing also baryon asymmetry [28,29]) through right-handed neutrino decays. The lepton number density to the entropy density in the limit $T_r < M_1 \equiv M_N \le m_{\rm inf}/2 \le M_{2,3}$ is defined as

$$\frac{n_L}{s} \sim \frac{3}{2}\frac{T_r}{m_{\rm inf}}\epsilon_{cp}, \tag{35}$$

where ϵ_{cp} is the CP asymmetry factor and is generated from the out of equilibrium decay of the lightest right-handed neutrino and is given by [43],

$$\epsilon_{cp} = -\frac{3}{8\pi}\frac{1}{(y_\nu y_\nu{}^\dagger)_{11}}\sum_{i=2,3}\mathrm{Im}[(y_\nu y_\nu{}^\dagger)_{1i}]^2\frac{M_N}{M_i}, \tag{36}$$

and T_r is the reheating temperature which can be as estimated as

$$T_r \simeq \sqrt{4}\frac{90}{\pi^2 g_\star}\sqrt{\Gamma m_P}, \tag{37}$$

where $g_\star$ is 228.75 for MSSM. The Γ is the decay width for the inflaton decay into right-handed neutrinos and is given by [43]

$$\Gamma(\mathrm{inf} \to N^c_iN^c_j) = \frac{1}{8\pi}\left(\frac{M_N}{M}\right)^2 m_{\rm inf}\left(1-\frac{4M_N^2}{m_{\rm inf}^2}\right)^{1/2}, \tag{38}$$

with the inflaton mass given by

$$m_{\rm inf} = \sqrt{2\kappa^2M^2 + M_S^2}. \tag{39}$$

Assuming a normal hierarchical pattern of light neutrino masses, the CP asymmetry factor, ϵ_{cp}, becomes

$$\epsilon_{cp} = \frac{3}{8\pi}\frac{M_N m_{\nu_3}}{v_u^2}\delta_{\rm eff}, \tag{40}$$

where m_{ν_3} is the mass of the heaviest light neutrino, $v_u = \langle H_u\rangle$ is the VEV of the up-type electroweak Higgs and $\delta_{\rm eff}$ is the CP-violating phase. The experimental value of lepton asymmetry is estimated as [44]

$$|n_L/s| \approx (2.67\text{–}3.02)\times 10^{-10}. \tag{41}$$

In the numerical estimates discussed below we take $m_{\nu_3} = 0.05$ eV, $|\delta_{\rm eff}| = 1$, and $v_u = 174$ GeV, while assuming large $\tan\beta$. The nonthermal production of lepton asymmetry n_L/s is given by the expression

$$\frac{n_L}{s} \lesssim 3\times 10^{-10}\frac{T_r}{m_{\rm inf}}\left(\frac{M_N}{10^6\ \mathrm{GeV}}\right)\left(\frac{m_{\nu_3}}{0.05\ \mathrm{eV}}\right), \tag{42}$$

with $M_1 \gg T_r$. Using the experimental value of $n_L/s \approx 2.5\times 10^{-10}$ with Eqs. (37) and (42), we obtain the following lower bound on T_r,

$$T_r \gtrsim 1.9\times 10^7\ \mathrm{GeV}\left(\frac{m_{\rm inf}}{10^{11}\ \mathrm{GeV}}\right)^{3/4} \times\left(\frac{10^{16}\ \mathrm{GeV}}{M_N}\right)^{1/2}\left(\frac{m_{\nu_3}}{0.05\ \mathrm{eV}}\right)^{1/2}. \tag{43}$$

A successful baryogenesis is usually generated through the sphaleron processes where an initial lepton asymmetry n_L/s is partially converted into a baryon asymmetry [45,46]. However, the right-handed neutrinos produced in inflaton decays are highly boosted, which affects the estimate of the final baryon asymmetry as given in [32]. Equation (43) is used in our numerical analysis to calculate inflationary predictions which are consistent with leptogenesis and baryogenesis.

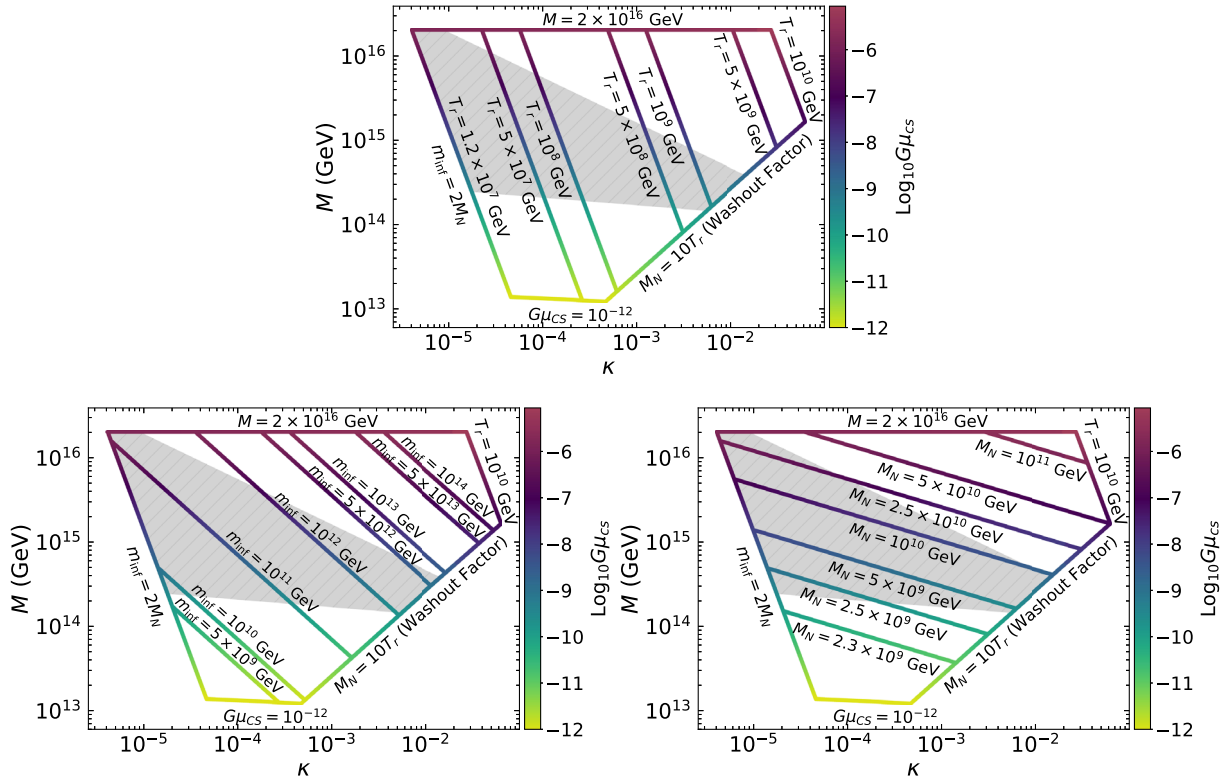

FIG. 2. Contours of the reheat temperature T_r (top), the inflaton mass $m_{\rm inf}$ (bottom left), and the right-handed neutrino mass M_N (bottom right), in the κ–M plane, where M is the $B-L$ gauge symmetry breaking scale. The boundary is drawn for different constraints shown. The color bar on the right displays the range of string tension parameter $G\mu_{CS}$. The shaded region represents the parametric space that is consistent with gravitino dark matter.

Figure 2 shows the contours of reheating temperature T_r (top), inflaton mass $m_{\rm inf}$ (bottom left), and right-handed neutrino mass M_N (bottom right) in κ–M plane. We obtain these parameters in the following ranges

$$\begin{aligned}&(10^7 \lesssim T_r \lesssim 10^{10})\ \text{GeV},\\ &(4.7\times 10^8 \lesssim M_N \lesssim 5.3\times 10^{11})\ \text{GeV},\\ &(9.4\times 10^8 \lesssim m_{\rm inf} \lesssim 7.6\times 10^{14})\ \text{GeV}.\end{aligned} \tag{44}$$

The color bar on the right displays the range of string tension parameter $G\mu_{CS}$, while the shaded region corresponds to the stable gravitino, as discussed in the following section.

C. Gravitino dark matter

An important constraint on the reheat temperature T_r arises, when gravitino cosmology is taken into account, that depends on the SUSY breaking mechanism and the gravitino mass $m_{3/2}$. As noted in [25,47], one may consider the case of

(α) a stable LSP gravitino;

(β) unstable long-lived gravitino with mass $m_{3/2} < 25$ TeV;

(γ) unstable short-lived gravitino with mass $m_{3/2} > 25$ TeV.

We first consider the case of stable gravitino, in which case it is the lightest SUSY particle (LSP) and assuming it is thermally produced, its relic density is estimated to be [48]

$$\Omega_{3/2}h^2 = 0.08\left(\frac{T_r}{10^{10}\ \text{GeV}}\right)\left(\frac{m_{3/2}}{1\ \text{TeV}}\right)\left(1+\frac{m_{\tilde g}^2}{3m_{3/2}^2}\right), \tag{45}$$

where $m_{\tilde g}$ is the gluino mass parameter and h is the present Hubble parameter in units of 100 km sec^{-1} Mpc^{-1} and $\Omega_{3/2}=\rho_{3/2}/\rho_c$.[1,2] A stable LSP gravitino requires $m_{\tilde g} > m_{3/2}$ while current LHC bounds on the gluino mass are around 2.2 TeV [52]. It is found from Eq. (45) that the overclosure limit $\Omega_{3/2} < 1$ puts a severe upper bound on

[1] $\rho_{3/2}$ and ρ_c are the present energy density of the gravitino and the critical energy density of the present universe, respectively.

[2] Equation (45) contains only the dominant QCD contributions for the gravitino production rate. In principle there are extra contributions descending from the electroweak sector as mentioned in [49,50] and recently revised in [51]. If we consider these types of contributions in our analysis, we estimate that (depending on gaugino universality condition) our results will deviate ∼(10–15)%.

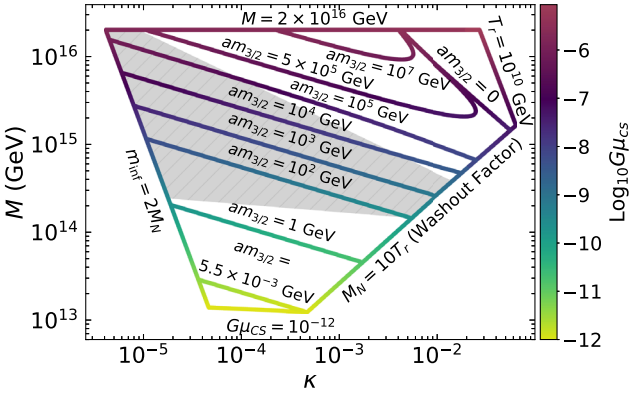

FIG. 3. Contours of the gravitino mass $m_{3/2}$ in the κ–M plane, where M is the $B-L$ gauge symmetry breaking scale. The boundary is drawn for different constraints shown. The color bar on the right displays the range of string tension parameter $G\mu_{CS}$. The gray shaded region corresponds to the parametric space where the gravitino is LSP $(m_{\tilde{g}} > m_{3/2})$.

the reheating temperature T_r, depending on the gravitino mass $m_{3/2}$. Here, we have omitted the contribution from the decays of squarks and sleptons into gravitinos. Using the lower bound of relic abundance $\Omega_h^2 = 0.144$ [53] in the above equation, we display a gray shaded region in Fig. 3 that satisfies the condition $(m_{\tilde{g}} > m_{3/2})$ and hence, in this region, the gravitino is the lightest supersymmetric particle and acts as a viable dark matter candidate. For gravity mediated SUSY breaking, the constraints on gravitino mass and reheat temperature from BBN are [54]

$$T_r \lesssim 10^7 \text{ GeV} \quad \text{for } m_{3/2} = (100\text{–}5000) \text{ GeV},$$
$$T_r \sim (10^7\text{–}2.5 \times 10^9) \text{ GeV} \quad \text{for } m_{3/2} \geq 5000 \text{ GeV}. \quad (46)$$

The shaded region in Fig. 3 describes the gravitino dark matter and the value of gravitino mass varies in the range $1.5 \text{ GeV} \lesssim m_{3/2} \lesssim 4.2 \times 10^5$ GeV with reheat temperature $T_r \gtrsim 10^7$ GeV. However, the gravitino mass in the range $100 \text{ GeV} \lesssim m_{3/2} \lesssim 5000$ GeV requires a reheat temperature $T_r < 10^7$ GeV, which is not achieved in our model and therefore, this small range of $m_{3/2}$ is ruled out by BBN.

An unstable gravitino, could be either long-lived or a short-lived. The lifetime of a long-lived gravitino with mass $m_{3/2} < 25$ TeV is about $\tilde{\tau} \gtrsim 1$ sec. A long-lived gravitino leads to the cosmological gravitino problem [55] that originates due to the fast decay of gravitino which may affect the light nuclei abundances and thereby ruin the success of BBN theory. To avoid this problem, one has to take into account the BBN bounds [Eq. (46)] on the reheating temperature. Nevertheless for all range of $5000 \leq m_{3/2} \leq 25000$ GeV, a long-lived gravitino scenario is viable and consistent with the BBN bounds (46).

For short-lived gravitino, the BBN bounds on the reheating temperature are not effective and gravitino decays into the LSP neutralino $\tilde{\chi}_1^0$, for which the abundance is given by

$$\Omega_{\tilde{\chi}_1^0} h^2 \simeq 2.8 \times 10^{11} \times Y_{3/2} \left(\frac{m_{\tilde{\chi}_1^0}}{1 \text{ TeV}} \right), \quad (47)$$

where $Y_{3/2}$ is the gravitino yield and is defined as

$$Y_{3/2} \simeq 2.3 \times 10^{-12} \left(\frac{T_r}{10^{10} \text{ GeV}} \right). \quad (48)$$

Since the LSP neutralino density produced by gravitino decay should not exceed the observed DM relic density, choosing the upper bound of relic abundance $\Omega_{\tilde{\chi}_1^0} h^2 = 0.126$ and using equations (48) and (47), we find a relation between the reheating temperature T_r and $m_{\tilde{\chi}_1^0}$, given by

$$m_{\tilde{\chi}_1^0} \simeq 19.6 \left(\frac{10^{11} \text{ GeV}}{T_r} \right). \quad (49)$$

For gravity mediation scenario $m_{\tilde{\chi}_1^0} \geq 18$ GeV [56], which is easily satisfied in the current model. Therefore, the short-lived gravitino scenario is also a viable possibility in this model. The region above the shaded area in Fig. 3 corresponds to short-lived gravitino. Finally, we obtain the following ranges of string tension $G\mu_{CS}$ and gravitino mass for stable and unstable gravitinos consistent with BBN bounds,

$$10^{-9} \lesssim G\mu_{CS} \lesssim 8 \times 10^{-6},$$
$$(-3.2 \times 10^9 \lesssim am_{3/2} \lesssim 5 \times 10^8) \text{ GeV}. \quad (50)$$

In the next section, we analyze the stochastic gravitational wave spectrum, consistent with leptogenesis and gravitino cosmology.

D. Gravitational waves from cosmic strings

The superposition of GW sources, such as inflation, cosmic strings, and phase transition, would generate a stochastic GW background. The tensor perturbations upon horizon reentry give rise to the inflationary SGWB [15,16,57,58] which imprint a distinctive signature in the CMB B-mode polarization. The amplitude and scale dependence of the inflationary SGWB is parametrized via the tensor-to-scalar ratio r and the tensor spectral index n_T, which satisfy the inflationary consistency relation $r = -8n_T$ [59], within single-field and hybrid slow-roll models. Since $r \geq 0$, this requires $n_T \leq 0$ (red spectrum) [60]. With current constraints on tensor-to-scalar ratio r, the amplitude of the inflationary SGWB on PTA and interferometer scales is far too small to be detectable by these probes and would instead require a strong blue tilted $(n_T > 0)$ primordial tensor power spectrum [15]. For a detailed study on SGWBs from first-order phase transition associated with the spontaneous $U(1)_{B-L}$ gauge symmetry breaking, see Refs. [61–64].

In this section, we study SGWB spectra produced by the decay of the cosmic string network [10–13]. The breaking of $U(1)_{B-L}$ gauge symmetry generates a stable cosmic string network that can put severe bounds on model parameters. These bounds can be relaxed if the cosmic strings are metastable. The embedding of the $U(1)_{B-L}$ group in the $SO(10)$ GUT gauge group leads to production of metastable cosmic string network which can decay via the Schwinger production of monopole–antimonopole pairs, generating a stochastic gravitational wave background, in the range of ongoing and future gravitational wave experiments.

The MSSM matter superfields reside in the **16** (spinorial) representation, whereas the MSSM Higgs doublet reside in **10** representations of $SO(10)$. The $SO(10)$ symmetry breaking to MSSM gauge group is achieved by nonzero VEV of **45** multiplet;

$$SO(10) \xrightarrow{\langle \mathbf{45} \rangle} G_{\rm MSSM} \times U(1)_\chi \xrightarrow{\langle \mathbf{16} \rangle, \langle \bar{\mathbf{16}} \rangle} G_{\rm MSSM}, \quad (51)$$

where $G_{\rm MSSM} \equiv SU(3)_C \times SU(2)_L \times U(1)_Y$ is the MSSM gauge group. The $U(1)_\chi$ charge is defined as a linear combination of hypercharge Y and $B-L$ charge,

$$Q_\chi = Yx + Q_{B-L}, \quad (52)$$

with x being a real constant. As a special case of $x=0$, the model, after spontaneous breaking of $SO(10)$, can be effectively realized as $B-L$ extended MSSM, $U(1)_{\chi=B-L}$. The Higgs superfield pair $(H, \bar{H})$ belong to $(\mathbf{16}+\bar{\mathbf{16}})$ representation of $SO(10)$ and is responsible for breaking G_{B-L} to MSSM. The first step gauge symmetry breaking produces magnetic monopoles which are inflated away during inflation, whereas the second step breaking produces metastable cosmic string network.

If cosmic strings form after inflation, they exhibit a scaling behavior where the stochastic GW spectrum is relatively flat as a function of the frequency, and the amplitude is proportional to the string tension μ_{CS}. For our case, μ_{CS} can be written in term of M as [65]

$$\mu_{CS} = 2\pi M^2 y(\Upsilon), \quad y(\Upsilon) \approx \begin{cases} 1.04\Upsilon^{0.195}, & \Upsilon > 10^{-2}, \\ \frac{2.4}{\log[2/\Upsilon]}, & \Upsilon < 10^{-2}, \end{cases} \quad (53)$$

where $\Upsilon = \frac{\kappa^2}{2g^2}$ with $g=0.7$ for MSSM. The CMB bound on cosmic string tension, reported by Planck 2018 [66,67] is

$$G\mu_{CS} \lesssim 2.4 \times 10^{-7}, \quad (54)$$

where $G\mu_{CS}$ denotes the dimensionless string tension with the gravitational constant $G = 6.7 \times 10^{-39}$ GeV^{-2}. The observation of GWs from cosmic strings is crucially dependent on two scales; the energy scale of inflation $\Lambda_{\rm inf}$, and the scale at which cosmic strings generate the GW spectrum $\Lambda_{CS} \equiv \sqrt{\mu_{CS}}$. The amplitude of the tensor mode cosmic microwave background anisotropy fixes the energy scale of inflation as $\Lambda_{\rm inf} \sim V^{1/4} \sim 3.3 \times 10^{16} r^{1/4}$ [68]. Using Planck 2σ bounds on tensor-to-scalar ratio r we obtain the upper limit on the scale of inflation, $\Lambda_{\rm inf} < 1.6 \times 10^{16}$ GeV [69]. In our model, strings form after inflation, namely, $\Lambda_{\rm inf} > \Lambda_{CS}$, for which a stochastic gravitational wave background is generated from undiluted strings. The SGWB arising from metastable cosmic string networks are expressed relative to critical density as [70]

$$\Omega_{\rm GW}(f) = \frac{\partial \rho_{\rm gw}(f)}{\rho_c \partial \ln f} = \frac{8\pi f (G\mu_{CS})^2}{3H_0^2} \sum_{n=1}^{\infty} C_n(f) P_n, \quad (55)$$

where $\rho_{\rm gw}$ denotes the GW energy density, ρ_c is the critical energy density of the Universe, and $H_0 = 100h$ km s^{-1} Mpc^{-1} is the Hubble parameter. The parameter $P_n \simeq \frac{50}{\zeta(4/3) n^{4/3}}$ is the power spectrum of GWs emitted by the nth harmonic of a cosmic string loop and $C_n(f)$ indicates the number of loops emitting GWs that are observed at a given frequency f

$$C_n(f) = \frac{2n}{f^2} \int_{z_{\rm min}}^{z_{\rm max}} dz \frac{\mathcal{N}(\ell(z), t(z))}{H(z)(1+z)^6}, \quad (56)$$

which is a function of number density of cosmic string loops $\mathcal{N}(\ell, t)$, with $\ell = 2n/((1+z)f)$. For the number density of cosmic string loops $\mathcal{N}(\ell, t)$ we use the approximate expressions of Blanco-Pillado-Olum-Shlaer (BOS) model given in [70,71]

$$\mathcal{N}_r(\ell, t) = \frac{0.18}{t^{3/2}(\ell + \Gamma G\mu_{CS} t)^{5/2}}, \quad (57)$$

$$\mathcal{N}_{m,r}(\ell, t) = \frac{0.18\sqrt{t_{eq}}}{t^2(\ell + \Gamma G\mu_{CS} t)^{5/2}} = \frac{0.18(2H_0\sqrt{\Omega_r})^{3/2}}{(\ell + \Gamma G\mu_{CS} t)^{5/2}} (1+z)^3. \quad (58)$$

For our region of interest, the dominant contribution is obtained from the loops generated during the radiation-dominated era. For $t(z)$ and $H(z)$, we use the expressions for ΛCDM cosmology assuming a standard thermal history of the Universe, while ignoring the changes in the number of effective degrees of freedom with z,

$$H(z) = H_0 \sqrt{\Omega_\Lambda + \Omega_m (1+z)^3 + \Omega_r (1+z)^4}, \quad (59)$$

$$t(z) = \int_{z_{\rm min}}^{z_{\rm max}} \frac{dz'}{H(z')(1+z')}, \qquad l(z) = \frac{2n}{(1+z)f}. \quad (60)$$

The integration range in the above equation corresponds to the lifetime of the cosmic string network, from its formation at $z_{\rm max} \simeq \frac{T_r}{2.7K}$ until its decay at $z_{\rm min}$ given by [72–74],

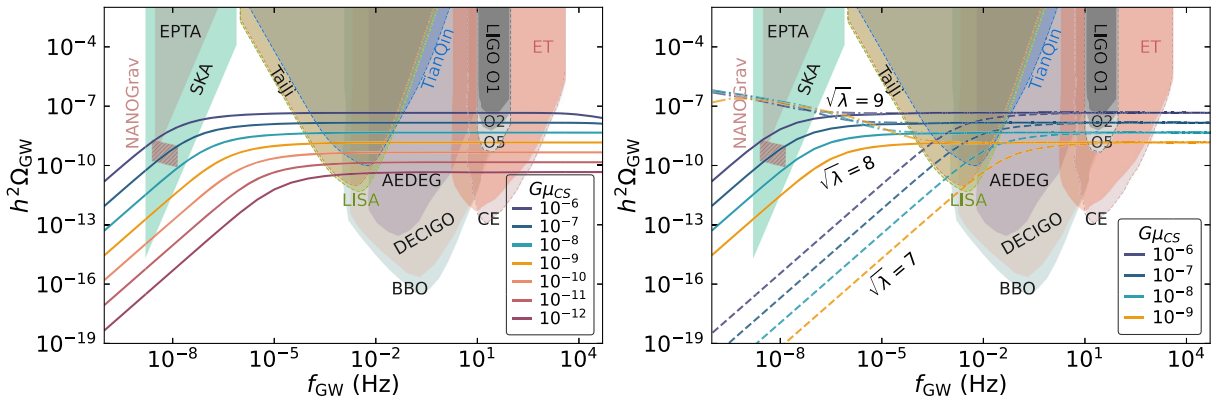

FIG. 4. Gravitational wave spectra from metastable cosmic strings explaining the NANOGrav excess at 2σ confidence level. The curves in the left panel are drawn for all ranges of string tension obtained in the model with $\sqrt{\lambda} = 8$. The curves in the right panel are drawn for the range of string tension consistent with nonthermal leptogenesis and gravitino dark matter, with $\sqrt{\lambda} = 7, 8, 9$. The shaded areas in the background indicate the sensitivities of the current and future experiments.

$$z_{\min} = \left(\frac{70}{H_0}\right)^{1/2} (\Gamma\Gamma_d G\mu_{CS})^{1/4}, \quad \Gamma_d = \frac{\mu}{2\pi} e^{-\pi\lambda}, \quad \lambda = \frac{m_M^2}{\mu}, \tag{61}$$

where $\Gamma \simeq 50$, m_M is the monopole mass, μ is the string tension, and we fix the reheat temperature at $T_r = 10^8$ GeV. The dimensionless parameter λ is the hierarchy between the GUT and $U(1)_{B-L}$ breaking scales. Figure 4 shows gravitational wave spectra from metastable cosmic strings for the predicted range of cosmic string tension, $10^{-12} \lesssim G\mu_{CS} \lesssim 10^{-6}$. The curves in left panel are drawn for the GUT and the $B-L$ breaking scales ratio, $\sqrt{\lambda} = 8$. The parametric space consistent with successful reheating with nonthermal leptogenesis and gravitino dark matter restricts the value of $G\mu_{CS}$ in the range $10^{-9} \lesssim G\mu_{CS} \lesssim 10^{-6}$. This is shown in the right panel of Fig. 4 where the curves are drawn for $\sqrt{\lambda} = 7, 8, 9$. It can be seen that the GW spectrum for the entire range of $G\mu_{CS}$ passes through most GW detector sensitivities. LIGO O1 [22] has excluded cosmic strings formation at $G\mu_{CS} \lesssim 10^{-6}$ in the high frequency regime 10–100 Hz. The low frequency band, 1–10 nHz, can be probed by NANOGrav [75], EPTA [76], and other GW experiments at nano Hz frequencies. Planned pulsar timing arrays SKA [77], space-based laser interferometers LISA [23], Taiji [78], TianQin [79], BBO [80], DECIGO [81], ground-based interferometers, such as Einstein Telescope [82] (ET), Cosmic Explorer [83] (CE), and atomic interferometer AEDGE [84], will probe GW generated by metastable cosmic string in a wide regime of frequencies.

E. Explaining the NANOGrav results

We now discuss the SGWB signal predicted by metastable cosmic strings for recent NANOGrav 12.5-yr results [75], which constrain the amplitude and slope of a stochastic process. The amplitude of the SGWB is obtained in terms of dimensionless characteristic strain $h_c = A(f/f_{\rm yr})^{\alpha}$ at the reference frequency $f_{\rm yr} = 32$ nHz as [12]

$$\Omega_{\rm GW}(f) = \frac{2\pi^2 f_{\rm yr}^2 A^2}{3H_0^2} \left(\frac{f}{f_{\rm yr}}\right)^{2\alpha+2} \equiv \Omega_{\rm gw}^{\rm yr} \left(\frac{f}{f_{yr}}\right)^{n_{gw}}, \tag{62}$$

where A is the strain amplitude. At low GW frequency, $\Omega_{\rm GW}$ behaves as $\sim f^{3/2}$, whereas at high GW frequencies, $\Omega_{\rm GW} \sim 1$. NANOGrav uses a power law fit with $5 - \gamma = 2 + 2\alpha = n_{gw}$ and constrain the parameters A and γ. This allows us to directly translate the 1σ and 2σ NANOGrav bounds given in [75] into the $\Omega_{\rm gw}^{\rm yr}$–$n_{\rm gw}$ plane, as displayed by the yellow shaded regions in Fig. 5. Following [11], we extract the amplitude $\Omega_{\rm gw}^{\rm yr}$ and slope $n_{\rm gw}$ using Eq. (62) by comparing the amplitude at the pivot scale f_* and taking the logarithmic derivative of $\Omega_{\rm gw}(f)$ at the desired frequency scale f_*,[3]

$$n_{\rm gw} = \left.\frac{d\log\Omega_{\rm GW}(f)}{d\log f}\right|_{f=f_*}, \tag{63}$$

$$\Omega_{\rm gw}^{\rm yr} = \Omega_{\rm GW}(f_*)\left(\frac{f_{\rm yr}}{f_*}\right)^{n_{\rm gw}}. \tag{64}$$

Figure 5 shows the comparison of the predictions from metastable cosmic strings (mesh of solid and dotted curves) with the constraints on the amplitude and tilt from [75] (yellow shaded region). We vary $G\mu_{CS}$ from 10^{-11} to 10^{-6}, however, the CMB constraint $G\mu_{CS} \leq 1.3 \times 10^{-7}$ only applies to cosmic strings with a lifetime exceeding CMB decoupling, corresponding to $\sqrt{\lambda} \gtrsim 8.6$. For each value of $G\mu_{CS}$, we consider the GUT and the $B-L$ breaking scales ratio in the range $\sqrt{\lambda} = 7.4$–9.0, where smaller values lead to a small spectrum at nHz frequencies that can be detected

[3]Here we have employed the numerical differentiation method. For the least squares power-law fit method, see [12].

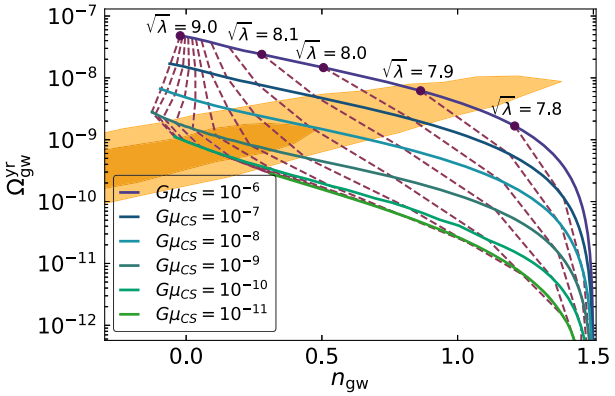

FIG. 5. Gravitational wave signals from metastable cosmic strings compared to the NANOGrav observations for different values of the string tension $G\mu_{CS}$ and the hierarchy between the GUT and $U(1)$ breaking scale λ. The solid colored lines represent fixed values of $G\mu_{CS}$ whereas the dotted lines represent contours of $\sqrt{\lambda}$. The dark (light) yellow region represent the 1σ (2σ) bounds reported by NANOGrav 12.5-yr data [75].

by future experiments, while all values $\sqrt{\lambda} \gtrsim 8.8$ quickly converge towards the result for stable cosmic strings and can be observed by NANOGrav and PPTA experiments [75]. The parametric space in the above model, consistent with successful reheating with nonthermal leptogenesis and gravitino dark matter restrict the allowed values of string tension to the range $10^{-9} \lesssim G\mu_{CS} \lesssim 8 \times 10^{-6}$ that lies within the 1σ and 2σ bounds of NANOGrav, as well as the sensitivity bounds of future gravitational wave experiments.

V. SUMMARY

To summarize, we have investigated various cosmological implications of a generic model based on the $U(1)_{B-L}$ extension of the MSSM gauge symmetry in a no-scale Kähler potential setup, highlighting the issues of inflation, leptogenesis, and baryogenesis gravitino as well as the stochastic gravitational wave background from metastable cosmic sting network. The embedding of $U(1)_{B-L}$ into a simply connected group $SO(10)$ produces a metastable cosmic string due to the spontaneous pair creation of a monopole and an antimonopole, which can generate a stochastic gravitational wave background in the range of ongoing and future gravitational wave experiments. The interaction between $U(1)_{B-L}$ Higgs and the neutrino superfields generate heavy Majorana masses for the right-handed neutrinos. The heavy Majorana masses explain the tiny neutrino masses via the seesaw mechanism, a realistic scenario for reheating and nonthermal leptogenesis. A wide range of reheat temperature $(10^7 \lesssim T_r \lesssim 10^{10})$ GeV and $U(1)_{B-L}$ symmetry breaking scale $(1.3 \times 10^{13} \lesssim M \lesssim 2.0 \times 10^{16})$ GeV is achieved here with successful nonthermal leptogenesis and stable gravitino as a possible dark matter candidate. The metastable cosmic string network admits string tension values in the range $10^{-12} \lesssim G\mu_{CS} \lesssim 8 \times 10^{-6}$. A successful reheating with nonthermal leptogenesis and gravitino dark matter restrict the allowed values of string tension to the range $10^{-9} \lesssim G\mu_{CS} \lesssim 8 \times 10^{-6}$, predicting a stochastic gravitational-wave background that lies within the 1σ bounds of the recent NANOGrav 12.5-yr data, as well as within the sensitivity bounds of future GW experiments.

ACKNOWLEDGMENTS

We thank Valerie Domcke, George K. Lenotaris, and Kazunori Kohri for valuable discussions. The work of S. N. is supported by the United Arab Emirates University under UPAR Grant No. 12S004.

[1] A. Vilenkin, Phys. Rep. **121**, 263 (1985).
[2] A. Vilenkin and E. P. S. Shellard, *Cosmic Strings and Other Topological Defects* (Cambridge University Press, Cambridge, England, 2000).
[3] P. Bhattacharjee, C. T. Hill, and D. N. Schramm, Phys. Rev. Lett. **69**, 567 (1992).
[4] C. T. Hill, Nucl. Phys. **B224**, 469 (1983).
[5] T. W. B. Kibble, J. Phys. A **9**, 1387 (1976).
[6] G. 't Hooft, Nucl. Phys. **B79**, 276 (1974).
[7] M. B. Hindmarsh and T. W. B. Kibble, Rep. Prog. Phys. **58**, 477 (1995).
[8] G. R. Dvali, Q. Shafi, and R. K. Schaefer, Phys. Rev. Lett. **73**, 1886 (1994).
[9] R. Jeannerot, J. Rocher, and M. Sakellariadou, Phys. Rev. D **68**, 103514 (2003).
[10] S. F. King, S. Pascoli, J. Turner, and Y. L. Zhou, Phys. Rev. Lett. **126**, 021802 (2021).
[11] John Ellis and Marek Lewicki, Phys. Rev. Lett. **126**, 041304 (2021).
[12] W. Buchmuller, V. Domcke, and K. Schmitz, Phys. Lett. B **811**, 135914 (2020).
[13] S. F. King, S. Pascoli, J. Turner, and Y. L. Zhou, J. High Energy Phys. 10 (2021) 225.
[14] W. Ahmed, M. Junaid, and U. Zubair, arXiv:2109.14838.
[15] S. Vagnozzi, Mon. Not. R. Astron. Soc. **502**, L11 (2021).
[16] M. Benetti, L. L. Graef, and S. Vagnozzi, Phys. Rev. D **105**, 043520 (2022).
[17] G. Lazarides, R. Maji, and Q. Shafi, Phys. Rev. D **104**, 095004 (2021).

[18] R. Samanta and S. Datta, J. High Energy Phys. 05 (2021) 211.
[19] S. Blasi, V. Brdar, and K. Schmitz, Phys. Rev. Lett. **126**, 041305 (2021).
[20] A. Ashoorioon, K. Rezazadeh, and A. Rostami, arXiv: 2202.01131.
[21] A. Ahriche, K. Hashino, S. Kanemura, and S. Nasri, Phys. Lett. B **789**, 119 (2019).
[22] B. P. Abbott *et al.* (LIGO Scientific and Virgo Collaborations), Phys. Rev. D **100**, 061101 (2019).
[23] P. Amaro-Seoane *et al.* (LISA Collaboration), arXiv: 1702.00786.
[24] B. Goncharov, R. M. Shannon, D. J. Reardon, G. Hobbs, A. Zic, M. Bailes, M. Curylo, S. Dai, M. Kerr, M. E. Lower *et al.*, Astrophys. J. Lett. **917**, L19 (2021).
[25] W. Ahmed, A. Karozas, and G. K. Leontaris, Phys. Rev. D **104**, 055025 (2021).
[26] W. Buchmuller, V. Domcke, and K. Schmitz, Nucl. Phys. **B862**, 587 (2012).
[27] W. Ahmed, S. Raza, Q. Shafi, C. S. Un, and B. Zhu, J. High Energy Phys. 01 (2021) 161.
[28] M. Fukugita and T. Yanagida, Phys. Lett. B **174**, 45 (1986).
[29] M. Flanz, E. A. Paschos, and U. Sarkar, Phys. Lett. B **345**, 248 (1995); **384**, 487(E) (1996); **382**, 447(E) (1996).
[30] S. Vagnozzi, E. Giusarma, O. Mena, K. Freese, M. Gerbino, S. Ho, and M. Lattanzi, Phys. Rev. D **96**, 123503 (2017).
[31] S. Vagnozzi, S. Dhawan, M. Gerbino, K. Freese, A. Goobar, and O. Mena, Phys. Rev. D **98**, 083501 (2018).
[32] W. Buchmuller, V. Domcke, H. Murayama, and K. Schmitz, Phys. Lett. B **809**, 135764 (2020).
[33] M. A. Masoud, M. U. Rehman, and Q. Shafi, J. Cosmol. Astropart. Phys. 11 (2021) 022.
[34] A. D. Linde, Phys. Rev. D **49**, 748 (1994).
[35] E. J. Copeland, A. R. Liddle, D. H. Lyth, E. D. Stewart, and D. Wands, Phys. Rev. D **49**, 6410 (1994).
[36] A. D. Linde and A. Riotto, Phys. Rev. D **56**, R1841 (1997); V. N. Senoguz and Q. Shafi, Phys. Rev. D **71**, 043514 (2005); M. U. Rehman, Q. Shafi, and J. R. Wickman, Phys. Lett. B **683**, 191 (2010).
[37] R. Jeannerot, S. Khalil, G. Lazarides, and Q. Shafi, J. High Energy Phys. 10 (2000) 012.
[38] G. Lazarides and C. Panagiotakopoulos, Phys. Rev. D **52**, R559 (1995).
[39] W. Ahmed, A. Karozas, G. K. Leontaris, and U. Zubair, arXiv:2201.12789.
[40] A. Afzal, W. Ahmed, M. U. Rehman, and Q. Shafi, arXiv:2202.07386.
[41] W. Buchmüller, V. Domcke, K. Kamada, and K. Schmitz, J. Cosmol. Astropart. Phys. 07 (2014) 054.
[42] J. Garcia-Bellido and A. D. Linde, Phys. Lett. B **398**, 18 (1997).
[43] K. Hamaguchi, arXiv:hep-ph/0212305.
[44] N. Aghanim *et al.* (Planck Collaboration), Astron. Astrophys. **641**, A6 (2020); **652**, C4(E) (2021).
[45] S. Y. Khlebnikov and M. E. Shaposhnikov, Nucl. Phys. **B308**, 885 (1988).
[46] J. A. Harvey and M. S. Turner, Phys. Rev. D **42**, 3344 (1990).
[47] G. Lazarides, M. U. Rehman, Q. Shafi, and F. K. Vardag, Phys. Rev. D **103**, 035033 (2021).
[48] M. Bolz, A. Brandenburg, and W. Buchmuller, Nucl. Phys. **B606**, 518 (2001).
[49] J. Pradler and F. D. Steffen, Phys. Rev. D **75**, 023509 (2007).
[50] V. S. Rychkov and A. Strumia, Phys. Rev. D **75**, 075011 (2007).
[51] H. Eberl, I. D. Gialamas, and V. C. Spanos, Phys. Rev. D **103**, 075025 (2021).
[52] T. A. Vami (ATLAS and CMS Collaboration), Proc. Sci., LHCP2019 (**2019**) 168.
[53] Y. Akrami *et al.* (Planck Collaboration), arXiv:1807.06211.
[54] M. Kawasaki, K. Kohri, and T. Moroi, Phys. Rev. D **71**, 083502 (2005); M. Kawasaki, K. Kohri, T. Moroi, and A. Yotsuyanagi, Phys. Rev. D **78**, 065011 (2008); M. Kawasaki, K. Kohri, T. Moroi, and Y. Takaesu, Phys. Rev. D **97**, 023502 (2018).
[55] M. Y. Khlopov and A. D. Linde, Phys. Lett. **138B**, 265 (1984).
[56] D. Hooper and T. Plehn, Phys. Lett. B **562**, 18 (2003).
[57] C. Caprini, J. Phys. Conf. Ser. **610**, 012004 (2015).
[58] S. Kuroyanagi, T. Takahashi, and S. Yokoyama, J. Cosmol. Astropart. Phys. 01 (2021) 071.
[59] A. R. Liddle and D. H. Lyth, Phys. Rep. **231**, 1 (1993).
[60] P. A. R. Ade *et al.* (BICEP2 and Keck Array Collaboration), Phys. Rev. Lett. **121**, 221301 (2018).
[61] R. Jinno and M. Takimoto, Phys. Rev. D **95**, 015020 (2017).
[62] T. Hasegawa, N. Okada, and O. Seto, Phys. Rev. D **99**, 095039 (2019).
[63] N. Haba and T. Yamada, Phys. Rev. D **101**, 075027 (2020).
[64] X. X. Dong, T. F. Feng, H. B. Zhang, S. M. Zhao, and J. L. Yang, J. High Energy Phys. 12 (2021) 052.
[65] C. T. Hill, H. M. Hodges, and M. S. Turner, Phys. Rev. Lett. **59**, 2493 (1987).
[66] P. A. R. Ade *et al.* (Planck Collaboration), Astron. Astrophys. **571**, A25 (2014).
[67] P. A. R. Ade *et al.* (Planck Collaboration), Astron. Astrophys. **594**, A13 (2016).
[68] R. Easther, W. H. Kinney, and B. A. Powell, J. Cosmol. Astropart. Phys. 08 (2006) 004.
[69] Y. Akrami *et al.* (Planck Collaboration), Astron. Astrophys. **641**, A10 (2020).
[70] J. J. Blanco-Pillado and K. D. Olum, Phys. Rev. D **96**, 104046 (2017).
[71] P. Auclair, J. J. Blanco-Pillado, D. G. Figueroa, A. C. Jenkins, M. Lewicki, M. Sakellariadou, S. Sanidas, L. Sousa, D. A. Steer, J. M. Wachter *et al.*, J. Cosmol. Astropart. Phys. 04 (2020) 034.
[72] L. Leblond, B. Shlaer, and X. Siemens, Phys. Rev. D **79**, 123519 (2009).
[73] A. Monin and M. B. Voloshin, Phys. Rev. D **78**, 065048 (2008).
[74] Wilfried Buchmuller, Valerie Domcke, and Kai Schmitz, Phys. Lett. B **811**, 135914 (2020); J. Cosmol. Astropart. Phys. 12 (2021) 006.
[75] Zaven Arzoumanian *et al.* (NANOGrav Collaboration), Astrophys. J. Lett. **905**, L34 (2020).
[76] R. D. Ferdman, R. van Haasteren, C. G. Bassa, M. Burgay, I. Cognard, A. Corongiu, N. D'Amico, G. Desvignes, J. W. T. Hessels, G. H. Janssen *et al.*, Classical Quantum Gravity **27**, 084014 (2010).

[77] R. Smits, M. Kramer, B. Stappers, D. R. Lorimer, J. Cordes, and A. Faulkner, Astron. Astrophys. **493**, 1161 (2009).
[78] W. R. Hu and Y. L. Wu, Natl. Sci. Rev. **4**, 685 (2017).
[79] J. Luo *et al.* (TianQin Collaboration), Classical Quantum Gravity **33**, 035010 (2016).
[80] V. Corbin and N. J. Cornish, Classical Quantum Gravity **23**, 2435 (2006).
[81] N. Seto, S. Kawamura, and T. Nakamura, Phys. Rev. Lett. **87**, 221103 (2001).
[82] M. Punturo, M. Abernathy, F. Acernese, B. Allen, N. Andersson, K. Arun, F. Barone, B. Barr, M. Barsuglia, M. Beker *et al.*, Classical Quantum Gravity **27**, 194002 (2010).
[83] B. P. Abbott *et al.* (LIGO Scientific Collaboration), Classical Quantum Gravity **34**, 044001 (2017).
[84] Y. A. El-Neaj *et al.* (AEDGE Collaboration), Eur. Phys. J. Quantum Technol. **7**, 6 (2020).